Title: Relaxation of Semiconductor Nanostructures using Molecular Dynamics with Analytic Bond Order

Corresponding Author: Dr Kurt Erich Scheerschmidt, Ph.D.

Corresponding Author's Institution: Max Planck Institute of Microstructure Physics

First Author: Kurt Scheerschmidt

Order of Authors: Kurt Scheerschmidt; Kurt Erich Scheerschmidt, Ph.D.; Volker Kuhlmann

Abstract: Molecular dynamics simulations using empirical potentials have been performed to describe atomic interactions during the relaxation of nanostructures. To include the quantum mechanical nature of atomic bonding a tight-binding based bond order potential (BOP) is developed applying analytically the first six moments. The BOP is improved using new on-site and π-terms of the local density of states. The applicability of the bond order potential and resulting enhancements in structural predictions are analyzed recalculating quantum dot relaxations and interface defects arising during bonding of two wafers with twist rotation misalignment. The most important property proposed by the extended BOP is an increased stiffness of the bonds which give modifications of local atomic arrangements near defects.

1

Relaxation of Semiconductor Nanostructures using Molecular Dynamics with Analytic Bond Order Potentials*

Kurt Scheerschmidt and Volker Kuhlmann

Max Planck Institute of Microstructure Physics,
Weinberg 2, D-06120 Halle, Germany
Email: *schee@mpi-halle.de*

Dedicated to Prof. Dr. H. Fischmeister on the occasion of his 80th birthday

Summary. Molecular dynamics simulations using empirical potentials have been performed to describe atomic interactions during the relaxation of nanostructures. To include the quantum mechanical nature of atomic bonding a tight-binding based bond order potential (BOP) is developed applying analytically the first six moments. The BOP is improved using new on-site and π-terms of the local density of states. The applicability of the bond order potential and resulting enhancements in structural predictions are analyzed recalculating quantum dot relaxations and interface defects arising during bonding of two wafers with twist rotation misalignment. The most important property proposed by the extended BOP is an increased stiffness of the bonds which give modifications of local atomic arrangements near defects.

1.1 Introduction

Molecular dynamics (MD) simulations [2] have been performed to study atomic processes related to the reordering at interfaces [3] and relaxation of nanostructures [4]. To enhance MD, we use the bond order potential (BOP) based on the tight binding (TB) model, as it preserves the essential quantum mechanical nature of atomic bonding. Just like *ab initio* methods, TB calculations require complete diagonalisation of the Hamiltonian, which scales as $\mathcal{O}(N^3)$ and restricts simulations to a few thousand atoms. The analytic BOP, however, achieves $\mathcal{O}(N)$ scaling by diagonalizing the orthogonal TB-Hamiltonian approximately and is recognized as a fast and accurate model for atomic interaction [5, 6, 7]. It allows to explore the dynamics of systems on macroscopic time and length scales on the atomic level that are beyond the realm of *ab initio* calculations. Such enhanced empirical TB based potentials make a sufficiently large number of particles and relaxation times up to μs accessible by MD including the electronic structure and the nature of the covalent bonds indirectly. The enhancement of the BOP is described in detail in [8, 9] and summarized in chapter 1.2. The ability of the BOP based MD is demonstrated here by comparing relaxations of quantum dots (cf. chapter 1.3) and interface structures (cf. chapter 1.4) with those using Tersoff potentials.

---

* Extended contribution published at MMM2006[1]

1.2 Analytic bond order potentials up to six moments

The approximations to develop analytic BOP potentials from DFT may be summarized by the following steps (for details cf. [5, 6, 7] and for the extensions cf. [8, 9]): construct the TB matrix elements by Slater-Koster two-centre integrals including s- and p- orbitals, transform the matrix to the bond representation, replace the diagonalization by Lanczos recursion, obtain the momenta from the continued fraction representation of the Green function up to order n for an analytic BOPn potential. The total cohesive potential energy U_{coh} has three contributions: pair repulsion, promotion energy U_{prom}, and bond energy as excess of the band energy over the individual atomic interactions $U_{bond} = 2\sum_{i\alpha,j\beta}\Theta_{j\beta,i\alpha}H_{i\alpha,j\beta}$. In the BOP representation the matrix elements $H_{i\alpha,j\beta}$ are replaced by the Slater-Koster two-center integrals h_{ij} and the Goodwin-Skinner-Pettifor distance scaling function. The bond order $\Theta_{i\sigma,j\sigma}$ is equivalent to the electron density for which a concise analytical expression $\left[1 + \frac{N^2(\Phi_{2\sigma}^i + \Phi_{2\sigma}^j) + \Phi_{2\sigma}^i \Phi_{2\sigma}^j(2N + \triangle\Phi_{4\sigma})}{(N + \triangle\Phi_{4\sigma})^2}\right]^{-1/2}$ can be given that employs the normalized second and fourth moment $(\Phi_{2\sigma}, \Phi_{4\sigma})$ of the local density of electronic states and $\triangle\Phi_{4\sigma} = (\Phi_{4\sigma}^i + \Phi_{4\sigma}^j - \Phi_{2\sigma}^{i2} - \Phi_{2\sigma}^{j2})/(\Phi_{2\sigma}^i + \Phi_{2\sigma}^j)$, $N^2 = \triangle\Phi_{4\sigma} + \Phi_{2\sigma}^i \Phi_{2\sigma}^j$. The normalized second moment was given as a sum of intersite and on-site hopping terms

$$\Phi_{2\sigma}^i = \sum_{k(i)\neq j} g_{\sigma,jik}^2 \hat{\beta}_{\sigma,ik}^2 + \hat{\delta}_i^2, \tag{1.1}$$

the latter beeing proportional to the energy splitting between atomic s- and p-states,

$$\hat{\delta}_i^2 = p_{\sigma,i}(1 - p_{\sigma,i})(E_s - E_p)^2/\beta_{\sigma,ij}^2. \tag{1.2}$$

The contribution $\Phi_{4\sigma}$ to the 4th moment was given in terms of the matrix-elements of the tight binding Hamiltonian,

$$\Phi_{4\sigma}^i = \sum_{k(i)\neq j} \hat{\beta}_{ik}^4 g_{jik}^2 + \sum_{\substack{k(i)\neq j \\ l(k)\neq i,j}} \hat{\beta}_{ik}^2 \hat{\beta}_{kl}^2 g_{jik}^2 g_{ikl}^2 + \sideset{}{'}\sum_{k(i),l(i)\neq j} \hat{\beta}_{ik}^2 \hat{\beta}_{il}^2 g_{jik} g_{kil} g_{il}, \tag{1.3}$$

with the bond angle θ_{jik}, the angular function

$$g_{\sigma,jik} = 1 + (\cos\theta_{jik} - 1)p_{\sigma,i}, \tag{1.4}$$

reduced TB-parameters

$$p_{\sigma,i} = \frac{pp\sigma_{ii}}{|ss\sigma_{ii}| + pp\sigma_{ii}}, \tag{1.5}$$

and normalized hopping integrals according $\hat{\beta}_{ik} = \beta_{ik}/\beta_{ij}$ etc.

The resulting semi-empirical many body potential is transferable to describe phases and configurations not included in the parameter fit, a feature not found with other empirical potentials. Moreover, transferability extends to different kinds of materials, where only the parameter need to be refitted. In the implementation of the enhanced BOP4+ a number of angular terms are included that are related to certain π bonds between neighboring atoms and contribute up to 40%, but were neglected previously. Both contributions exhibit new angular dependencies, different from those

already accounted for in the expressions given in [5] and the second order BOP2 [10, 11]. With the torsional function

$$g_{\varphi,jl} = p_{\pi,ik}\sqrt{p_{\sigma,i}p_{\sigma,k}}\cos\varphi_{jl}\sin\theta_{jik}\sin\theta_{ikl}, \qquad (1.6)$$

this contribution reads

$$\sum_{k(i)\neq j}\sum_{l(k)\neq i,j}\hat{\beta}^2_{\sigma,ik}\hat{\beta}^2_{\sigma,kl}\left[2g_{\sigma,jik}g_{\sigma,ikl} + g_{\varphi,jl}\right]g_{\varphi,jl}. \qquad (1.7)$$

Similarly on-site contributions to $\Phi_{4\sigma}$ proportional to the energy splitting δ_i are included:

$$\sum\hat{\beta}^2_{ik}\left\{g_{jik}(2\hat{\delta}^2_i + \hat{\delta}^2_k) + \hat{p}_i(1-\hat{p}_i)\hat{\delta}^2_i(1-\theta_{jik})^2\right\} + \hat{\delta}^4_i. \qquad (1.8)$$

Besides an accurate fit, the BOP requires well parameterized TB matrix elements or parameter optimizing, and the problem of transferability have to be considered separately. For BOP of order n = 2 [10, 11] the bond-order term looks like a Tersoff potential and the numerical behavior of BOP2 and the empirical Tersoff potential are approximately equivalent. A detailed description of the enhanced analytical BOP4+ is given elsewhere [8, 9], together with the derivation of the individual terms and their importance to better describe the electronic origin for angular dependend bonding.

(a)

(b)
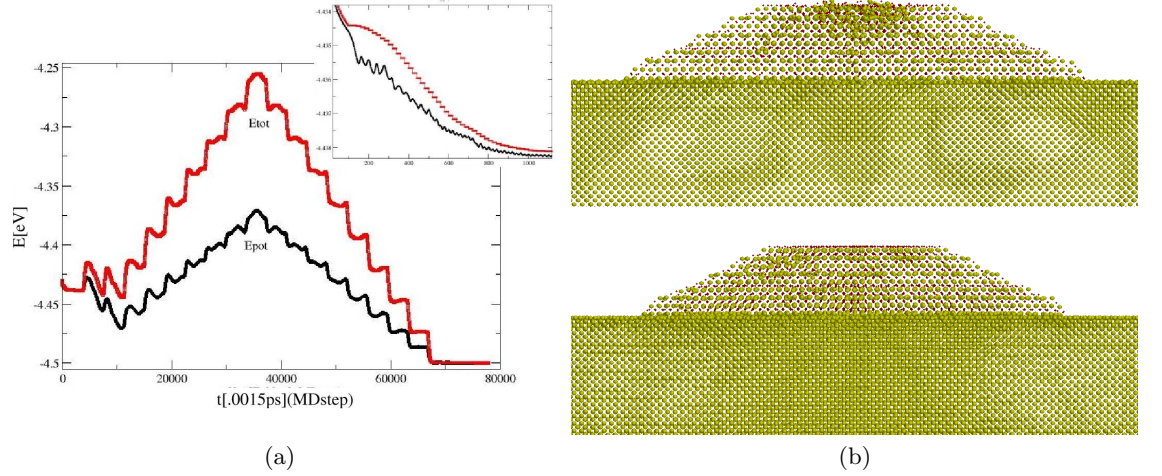
Fig. 1.1. MD relaxation of an SiGe/Si island: (a) Potential and total energy during annealing up to 900K, inset: enlarged first 1000 steps relaxing start configuration at 0K, (b) [110] views after annealing with a Tersoff potential (top) and an analytical BOP4+ (bottom).

1.3 BOP4+ in MD relaxation of quantum dots

A quantum dot (QD) is a nanometer scaled island or region of suitable material free-standing on or embedded in semiconductor or other matrices. Especially shape, size and strain field of single

QDs as well as quality, density, and homogeneity of equisized and equishaped dot arrangements are important features which control the optical properties, the emission and absorption of light, the lasing efficiency, etc. MD with suitable potentials allows to describe the relaxation and to predict structural properties of QDs.

Fig. 1.1 (a) shows the behavior of the potential and the total energy of a SiGe/Si-island and Fig. 1.1 (b) the structural difference after relaxing the system up to 900K with Tersoff and BOP4+ potentials, respectively. Due to the different nearest and next nearest neighbor relations - hopping matrix elements up to 6th order - the better stiffness of the BOP4+ yields better structural stability.
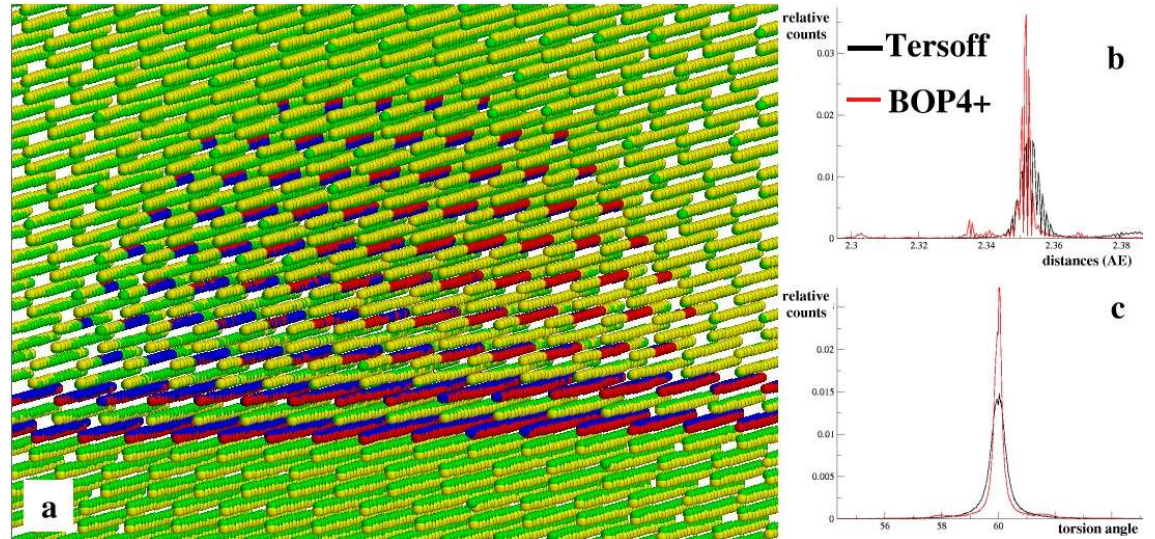
Fig. 1.2. MD relaxation up to 900K of an embedded SiGe pyramid in Si comparing Tersoff and BOP4+ potentials: (a) Relaxed atom positions for Tersoff (Si yellow, Ge red) and BOP4+ (Si green, Ge blue) with an slight overall shift to separate the 110-dumbbell rows, (b) pair distribution, and (c) distribution of the torsion angles.

Fig. 1.2 (a) shows the difference in lattice plane bending comparing the atomic positions after annealing an embedded truncated (001)-SiGe/Si quantum dot of pyramidal shape having 111 faccettes. The different bending of the atomic rows is demonstrated using different colors for Si and Ge after applying the Tersoff potential (yellow/red, resp.) and the enhanced BOP4+ (green/blue, resp.). Thus different strains are created especially within the QD, which also is reflected by the pair distribution in Fig. (b). The torsion angle distribution in Fig. (c), however, shows solely a sharper maximum around the 60° equilibrium angle indicating the higher stffness of the BOP4+.

1.4 BOP4+ in MD investigations of wafer bonded interfaces

Wafer bonding, i.e. the creation of interfaces by joining two wafer surfaces, has become an attractive method for many practical applications in microelectronics, micromechanics or optoelectronics. The

macroscopic properties of bonded materials are mainly determined by the atomic processes at the interfaces during the transition from adhesion to chemical bonding. Thus, the description of the atomic processes is of increasing interest to support the experimental investigations or to predict the bonding behavior. Whereas bonding of two perfectly aligned, identical wafers yields a single,
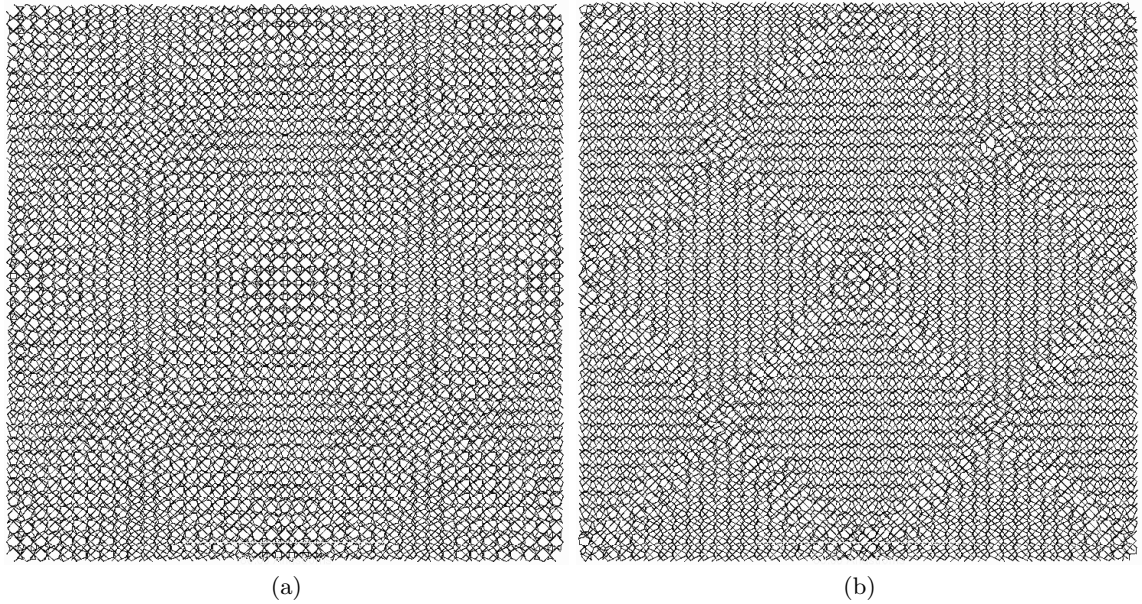
Fig. 1.3. MD simulated structural models of bonded wafers ([001] views, bond representation of 3 lattice planes around the interface) with rotationally 2.8° twist angles (134500 atoms, 22nm box) annealed at 900K for orthogonal dimer start configurations: (a) Tersoff potential; (b) BOP4+ potential.

perfectly bonded wafer without defects, miscut of the wafer results in steps on the wafer surfaces and thus edge dislocations at the bonded interfaces are created. Bonding wafers with rotational twist leads additionally to a network of screw dislocations at the interface, in dependence of the twist angle different bonding behavior is observed as discussed in detail, e.g., in [12]. A special situation is the 90° twist, e.g. between monoatomic steps, giving a (2x2) reconstructed interface and consisting of structural units called the $\overline{4}2m$-dreidl [13, 14, 15]. The dreidl structure is found to be also the minimum energy configuration in DFT-LDA simulations. All interface relaxations, however, are strongly influenced by the atomic potential model used, as it is demonstrated in Figs. 1.3-1.6 comparing MD interface simulations with Tersoff and BOP4+, respectively. Figs. 1.3 and 1.4 show the resulting minimum structures gained for higher annealing temperatures (900K) of a wafer bonded interface with a twist rotation of 2.8°. The [001]-projections of the bonds normal to the bonded interface up to next nearest neighbors is given in Figs. 1.3 (a) and (b) for the MD relaxation with Tersoff and BOP4+ potentials, respectively. In Fig. 1.4 the [110] projection is shown, with both the Tersoff and the BOP4+ simulation projected by different colors into the same view. One reveals the more located imperfectly bonded regions around the screw dislocations
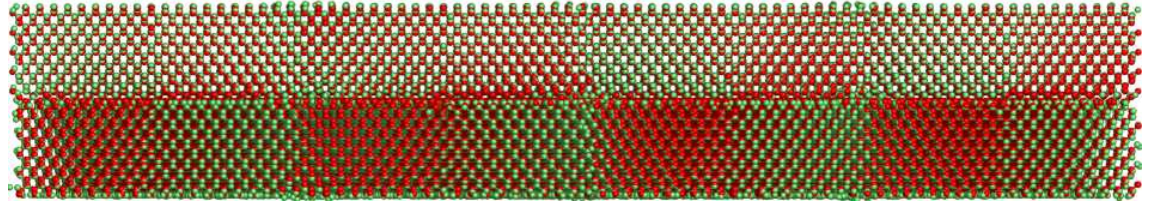
Fig. 1.4. MD relaxation of bonding rotationally twisted wafers ([110] view) with 2.8° angle, 22nm box, orthogonal dimers: structural difference using Tersoff (green) and BOP4+ potentials (red).

for the Tersoff potential, whereas the relaxation with BOP4+ yield more stability due to the higher potential stiffness according to the 6th moment hopping terms. Finally, in Fig. 1.5 the pair-, bond angle-, and torsion angle distributions are shown for the 2.8°-twist bonded interface, only 3 lattice planes around the interface are considered in distance and angle counting. The Tersoff potential yields the characteristic first and second neighbor distances as well as the bond angle of 109°. The calculation with the BOP4+ demonstrates the characteristic deviations due to the better description of the electronic bond structure. So, for instance, the Tersoff potential is defined without torsion, thus the corresponding distribution in Fig. 1.5 (c) has no relevant peaks. However, the angular distribution Fig. 1.5 (b) shows remarkable maxima at 95° and 125°.

(a)   (b)   (c)
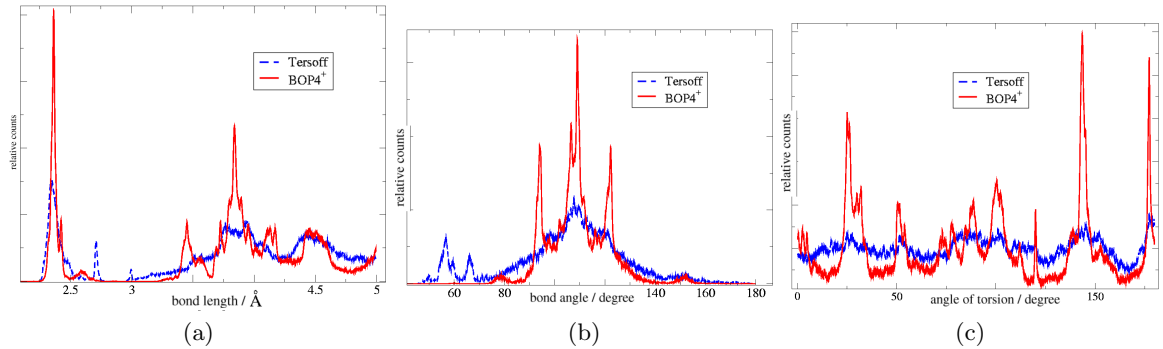
Fig. 1.5. Distribution functions for MD simulated structural models of bonded wafers with rotationally twist angle of 2.8° annealed at 900K assuming Tersoff potential (blue) and BOP4+ potential (red): (a) radial distribution function, (b) bond angles, and (c) torsion angles.

Fig.1.6 shows the interface region after bonding of 8.8° rotationally twisted (001)-Si wafers. The annealing at 900K rearranges the atomic configurations at the interfaces to screw dislocations with overlapping core regions, thus the atomic rows at the interface are bended nearly across the whole wafer. Contrary to the results for the 2.8° twist boundary, the peak of the pair distribution on the right hand side of Fig.1.6 is sharpened for the BOP4+ potential. Thus here for the overlapping core regions of the screw dislocations the higher stiffness of the potential yield a better relaxation of the bonded interface.
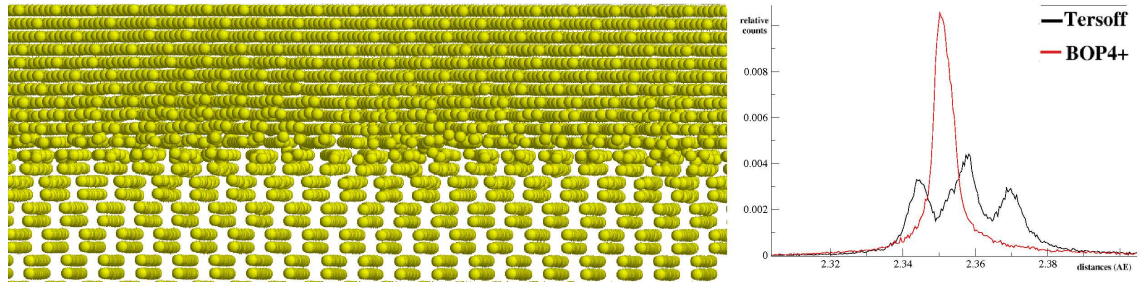
Fig. 1.6. MD relaxation of bonding rotationally twisted wafers with 8.8° angle, 11nm box, orthogonal dimers: (a) Interface region in approximately [110] view of the lower crystal part, (b) pair distribution of five adjacent layers around the interface.

1.5 Conclusions

Molecular dynamics simulations (MD) based on empirical potentials are used to investigate the relaxation of nanostructures. It is demonstrated that different final structures for different potentials occur in simulating, e.g., quantum dot relaxations or the bonding of two Si(001) wafers rotationally misaligned. The angular and distance behavior near defects shows the better electronic potential structure for the enhanced BOP4 potential. It clearly demonstrates the importance of enhanced empirical potentials as it is given by the tight-binding based analytic bond-order potential BOP4+ up to 6th order momenta.

References

1. K. Scheerschmidt and V. Kuhlmann, Proc. Multiscale Materials Modelling, MMM2006, Freiburg, 18.-22.9.2006, Ed. P. Gumbsch, pp. 102-105.
2. K. Scheerschmidt, Empirical Molecular Dynamics: Possibilities, Requirements and Limitations, in: *Theory of Defects in Semiconductors*, D.A. Drabold, S. Estreicher, Topics in Applied Physics, Springer Verlag 2006, Chapter 9, pp. 213-244.
3. K. Scheerschmidt and P. Werner, Characterization of Structure and Composition of Quantum Dots by Transmission Electron Microscopy, in: *Nano-Optoelectronics: Concepts, Physics and Devices*, Ed. M. Grundmann, Springer Verlag 2002, Chapter 3, pp. 67-98.
4. K. Scheerschmidt and V. Kuhlmann, Interface Science **12** (2004) 157.
5. A.P. Horsfield, A.M. Bratkovsky, M. Fearn, D.G. Pettifor, and M. Aoki, Phys. Rev. **B 53** (1996) 12694.
6. D.G. Pettifor, M.W. Finnis, D. Nguyen-Manh, D.A. Murdick, X.W. Zhou, and H.N.G. Wadley, Mater. Sci. Eng., **A 365** (2004) 2.
7. M.W. Finnis: *Interatomic Forces in Condensed Matter*, Oxford Series on Materials Modelling, Oxford University Press 2003.
8. V. Kuhlmann, Thesis, Martin-Luther-Universität, Halle 2006.
9. V. Kuhlmann and K. Scheerschmidt, Phys. Rev. B, (2007) in print.
10. D. Conrad and K. Scheerschmidt, Phys. Rev. B **58** (1998) 4538.
11. K. Scheerschmidt, D. Conrad, and A. Belov, Comput. Mater. Sci. **24** (2002) 33.
12. K. Scheerschmidt, MRS Proceedings Volume **681E** (2002), I2.3.
13. A.Y. Belov, D. Conrad, K. Scheerschmidt, and U. Gösele, Philos. Magazine A**77** (1998) 55.

14. A.Y. Belov, K. Scheerschmidt, and U. Gösele, phys. status solidi (a) **159** (1999) 171.

15. K. Scheerschmidt, D. Conrad, A. Belov, Comput. Mater. Sci. **24** (2002) 33 .

This is e-TeXk, Version 3.141592-2.1 (Web2c 7.5.2) (format=latex 2004.6.9) 19 APR 2007 10:09

entering extended mode

 %&-line parsing enabled.

 (c:/TeX/texmf/web2c/cp8bit.tcx)

**c:/pdfbuilder/temp/ruehle07.tex

(c:/pdfbuilder/temp/ruehle07.tex

LaTeX2e <2001/06/01>

Babel <v3.7j> and hyphenation patterns for english, dumylang, nohyphenation, ba

sque, czech, slovak, german, ngerman, danish, spanish, catalan, finnish, french

, ukenglish, greek, croatian, hungarian, italian, latin, mongolian, dutch, norw

egian, polish, portuguese, russian, ukrainian, serbocroat, swedish, loaded.

(./svmult.cls

Document Class: svmult 2004/05/18 v3.14

Springer Verlag global LaTeX document class for multi authored books

Class Springer-SVMult Warning: Specified option or subpackage "a4paper"

(Springer-SVMult)   not found passing it to article class

(Springer-SVMult)   - on input line 158.

Class Springer-SVMult Info: extra/valid Springer sub-package

(Springer-SVMult)   not found in option list - using "global" style.

(c:/TeX/texmf/tex/latex/base/article.cls

Document Class: article 2001/04/21 v1.4e Standard LaTeX document class

(c:/TeX/texmf/tex/latex/base/size10.clo

File: size10.clo 2001/04/21 v1.4e Standard LaTeX file (size option)

)

\c@part=\count79

\c@section=\count80

\c@subsection=\count81

\c@subsubsection=\count82

\c@paragraph=\count83

\c@subparagraph=\count84

\c@figure=\count85

\c@table=\count86

\abovecaptionskip=\skip41

\belowcaptionskip=\skip42

\bibindent=\dimen102

```
)
\betweenumberspace=\dimen103
\headlineindent=\dimen104
\minitoc=\write3
\c@minitocdepth=\count87
\c@chapter=\count88
\svitemindent=\dimen105
\verbatimindent=\dimen106
LaTeX Font Info:    Redeclaring math symbol \Gamma on input line 726.
LaTeX Font Info:    Redeclaring math symbol \Delta on input line 727.
LaTeX Font Info:    Redeclaring math symbol \Theta on input line 728.
LaTeX Font Info:    Redeclaring math symbol \Lambda on input line 729.
LaTeX Font Info:    Redeclaring math symbol \Xi on input line 730.
LaTeX Font Info:    Redeclaring math symbol \Pi on input line 731.
LaTeX Font Info:    Redeclaring math symbol \Sigma on input line 732.
LaTeX Font Info:    Redeclaring math symbol \Upsilon on input line 733.
LaTeX Font Info:    Redeclaring math symbol \Phi on input line 734.
LaTeX Font Info:    Redeclaring math symbol \Psi on input line 735.
LaTeX Font Info:    Redeclaring math symbol \Omega on input line 736.
\tocchpnum=\dimen107
\tocsecnum=\dimen108
\tocsectotal=\dimen109
\tocsubsecnum=\dimen110
\tocsubsectotal=\dimen111
\tocsubsubsecnum=\dimen112
\tocsubsubsectotal=\dimen113
\tocparanum=\dimen114
\tocparatotal=\dimen115
\tocsubparanum=\dimen116
\foot@parindent=\dimen117
\spthmsep=\dimen118
\c@theorem=\count89
\c@case=\count90
\c@conjecture=\count91
\c@corollary=\count92
\c@definition=\count93
\c@example=\count94
```

```
\c@exercise=\count95
\c@lemma=\count96
\c@note=\count97
\c@problem=\count98
\c@property=\count99
\c@proposition=\count100
\c@question=\count101
\c@solution=\count102
\c@remark=\count103
\instindent=\dimen119
\figgap=\dimen120
\figcapgap=\dimen121
\tabcapgap=\dimen122
\c@merk=\count104
\c@@inst=\count105
\c@@auth=\count106
\c@auco=\count107
\instindent=\dimen123
\authrun=\box26
\authorrunning=\toks14
\tocauthor=\toks15
\titrun=\box27
\titlerunning=\toks16
\toctitle=\toks17
\c@contribution=\count108
) (c:/TeX/texmf/tex/latex/base/flafter.sty
Package: flafter 2000/07/23 v1.2i Standard LaTeX floats after reference (FMi)
) (c:/TeX/texmf/tex/latex/graphics/graphicx.sty
Package: graphicx 1999/02/16 v1.0f Enhanced LaTeX Graphics (DPC,SPQR)
(c:/TeX/texmf/tex/latex/graphics/keyval.sty
Package: keyval 1999/03/16 v1.13 key=value parser (DPC)
\KV@toks@=\toks18
) (c:/TeX/texmf/tex/latex/graphics/graphics.sty
Package: graphics 2001/07/07 v1.0n Standard LaTeX Graphics (DPC,SPQR)
(c:/TeX/texmf/tex/latex/graphics/trig.sty
Package: trig 1999/03/16 v1.09 sin cos tan (DPC)
) (c:/TeX/texmf/tex/latex/texlive/graphics.cfg
```

File: graphics.cfg 2001/08/31 v1.1 graphics configuration of teTeX/TeXLive

)

Package graphics Info: Driver file: dvips.def on input line 80.

(c:/TeX/texmf/tex/latex/graphics/dvips.def

File: dvips.def 1999/02/16 v3.0i Driver-dependant file (DPC,SPQR)

))

\Gin@req@height=\dimen124

\Gin@req@width=\dimen125

)

! LaTeX Error: File `subeqnar.sty' not found.

Type X to quit or <RETURN> to proceed,

or enter new name. (Default extension: sty)

Enter file name:

! Emergency stop.

<read *>

l.11 ...aphicx} \usepackage{subeqnar} \setlength

                                        {\textwidth}{15.0 cm}^^M

*** (cannot \read from terminal in nonstop modes)

Here is how much of TeX's memory you used:

 994 strings out of 95104

 10681 string characters out of 1186615

 64838 words of memory out of 1517227

 4117 multiletter control sequences out of 10000+50000

 3640 words of font info for 14 fonts, out of 1000000 for 2000

 458 hyphenation exceptions out of 1000

 29i,0n,21p,603b,36s stack positions out of 5000i,500n,6000p,200000b,40000s

No pages of output.